

# Green's Function Refinement as an Approach to Radar Backscatter: General Theory and Applications to LGA Scattering from the Ocean

William T. Shaw and Andrew J. Dougan

**Abstract**— We present a new approach to the computation of radar returns from dielectric bodies whose boundary is the deformation of a plane surface. The method relies on combining a systematic improvement in the Green's function with a good approximate choice of local boundary condition. In this paper, the general theory is presented together with a simple application where the Green's function is that for a lossy dielectric half-space. We derive the root radar cross section (RCS) for a statistical surface and the mean backscatter RCS for a rough surface. We explore the applications to low-grazing-angle (LGA) scattering from statistical surfaces with an ocean-like spectrum and demonstrate that such a model explains some of the previously unexplained LGA phenomena, such as the absolute and relative levels of the vertical (VV) and horizontal (HH) channel RCS measurements.

**Index Terms**— Green's function, sea-surface electromagnetic scattering.

## I. INTRODUCTION

BACKSCATTER from surfaces at low-grazing angle (LGA) presents several puzzles for theoretical and numerical modelers. The nature of the problems depend to some extent on the context and the context of scattering from the ocean presents particular challenges. In this case, there are very basic problems to be resolved about the polarization sensitivity of both the radar cross section (RCS) and Doppler spectra. In a recent survey, Apel [1] cited one issue in particular—the fact that vertical (VV) returns from the ocean are very similar in level to those obtained via the small perturbation method (SPM), while the horizontal (HH) returns are significantly higher than the corresponding SPM value. Other issues have been described by Lee *et al.* [16] and Ward [34] and include “spikes” in the HH returns and dislocation of the Doppler spectra peaks in the two polarizations.

The purpose of this paper is to describe a new analytical model of scattering from a statistical surface that appears to capture at least some of these so far unexplained phenomena.

In analytical models, one assumes some form of approximate boundary condition and proceeds to evaluate a surface integral for the scattering. The scattering integral involves the far-field components of a Green's function. The vast majority of past work on this problem just uses the free-space Green's

function while substantial theoretical and numerical effort has gone into improving the estimate of the surface fields. But, if the exact Green's function for the problem were known, there would be no surface integral left to evaluate as the scattering is given by a volume integral involving the full Green's function and currents in the radar antenna source. DeSanto was the first to look at how the Green's function could be improved in his series of studies (in particular the electromagnetic analysis of [6]). But DeSanto focused only on the volume integral term involving a rough surface Green's function computed as an approximate diagrammatic solution to the Green's function integral equation in the perfectly conducting (PC) case C. Flammer [8] considered a perturbative approach to the PC case. More recently, an approach which combines elements of diagram theory and perturbation theory has been taken up by Mudaliar [19].

In recent years, a substantial program of numerical simulation has begun in several centers that aims to solve for the electromagnetic surface currents exactly. We cannot claim to be aware of all the threads that have been taken up in such approaches, but the work by Holliday *et al.* [11], [12], Kapp and Brown, [14], Kim *et al.* [15], Spivak [26], and Thorsos and Jackson [29] cover a range of methods including Volterra, “forward–backward,” and other approaches. These approaches have the advantage that it can be checked when the electromagnetic boundary conditions are satisfied, giving considerable confidence in the quality of the answer. It is also possible to investigate particular deterministic surfaces with relative ease. In contrast, in our approach we merely postulate an approximate boundary condition and live with its deficiencies. It is vital to appreciate that the purposes of Green's function refinement is to systematically render these deficiencies less significant, by making the mapping from surface electromagnetic (EM) currents to the RCS less and less sensitive to the errors in the assumed surface current. Our method is, therefore, complementary to the numerical approach over which it has the distinct advantages of being able to handle: 1) two-dimensional (2-D) surfaces (present numerical work, as far as we are aware, appears to be limited to one-dimensional (1-D) surfaces) and 2) a statistical description of the surface, thereby enabling meaningful discussion of the impact of the surface-wave spectrum on the RCS and its consequences for synthetic aperture radar (SAR) imagery and detection theory for internal waves and other disturbances. In principle, at least some of these numerical methods could be

Manuscript received February 20, 1997; revised August 20, 1997.

The authors are with Oxford System Solutions, The Magdalen Centre, Oxford Science Park, Oxford, OX4 4PQ U.K.

Publisher Item Identifier S 0018-926X(98)01033-3.

used to establish the domain of validity of the model we shall present here, very much in the spirit of [15] and [29].

We are certainly not alone in attempting to build a more accurate analytical model for statistical surfaces. A priority for our future studies must be to understand how our approach is related to other groups. The family of methods based on small-slope approximations developed by Tatarskii and Tatarskii [28] and Voronovich [32] is of particular interest, as it appears to have some features (such as “containing” in some form—theories of both Kirchhoff and SPM type) in common with our approach. We wish to point out that although we shall introduce our own form of small-slope approximation, denoted linear slope variation (LSV) and quadratic slope variation (QSV), it is a computational approximation introduced to extract tractable detailed answers. The notion of a small slope plays no *fundamental* role in our model.

There is a close relationship between our family of models, which are nonperturbative, and some existing models rooted in perturbation theory. It is possible to regard the Green’s function method as a nonperturbative extension of work by Burrows [5] and Mitzner [18] and it therefore offers the possibility of providing generalizations of the analysis by Brown [4]. Some clues as to how this works are given in the remarks at the end of Section IV, but a clear view of the correspondence relies on an analysis of reciprocity by Tough and Ward [30].

To give a better context to our own approach, let us enumerate some scenarios for the geometry associated with Green’s function and approximate boundary condition. First, the Green’s function geometry scenarios, labeled GF( $i$ ),  $i = 1-7$  are as follows:

- 1) free-space;
- 2) perfectly conducting (PC) flat plane;
- 3) flat plane bounding dielectric half-space;
- 4) perturbation of PC flat plane;
- 5) perturbation of planar surface bounding a dielectric;
- 6) fully rough PC surface;
- 7) fully rough boundary to dielectric.

Next, we list some approximate boundary conditions, BC( $i$ ),  $i = 1-7$  (of the analytically tractable variety):

- 1) perfectly conducting (unshadowed) Kirchhoff;
- 2) tangent-plane impedance Kirchhoff;
- 3) curvature-corrected impedance Kirchhoff;
- 4) perfectly conducting shadowed Kirchhoff;
- 5) impedance shadowed Kirchhoff;
- 6) curvature-corrected impedance shadowed Kirchhoff;
- 7) extended integral boundary condition.

Our general plan is to push down these two lists as far as possible. Some cases have been done. For example, Holliday *et al.* 1986 ocean-imaging model [10] is based on scenarios GF(1) + BC(1). An analysis of the combination GF(1) + BC(2) was developed by Hagfors [9]. A scalar version of GF(2) + BC(1) was developed by Berman and Perkins [2] and was extended by us to the electromagnetic case in [21]. These latter two models demonstrate very explicit consistency between the Kirchhoff approximation and first-order SPM, but in the electromagnetic case, the PC model predicts a VV/HH

ratio of just a few dB for LGA backscatter with surfaces that are PC but otherwise ocean like. However, in the PC model there are some oddities in the general absolute levels of the RCS and we wished to develop a corresponding dielectric model in order to remedy this. In this paper, for the first time we present an analysis of the combination of GF(3) with BC(2). We make brief comments on the extension to BC(3) and BC(7). We have not yet considered the combination of a refined Green’s function with shadowed boundary conditions BC(4-6) though this can be approached by combining what we have already with some form of geometric shadowing as defined, for example, by Brown [3], Smith [25], and Wagner [33]. A prototype could be based on the work of Sancer [20].

We shall show that the GF(3) + BC(2/3) models define a theory that contains both Kirchhoff theory and SPM theory for high-contrast lossy dielectric media. We shall combine the general form of the theory with an approximate simple model of the ocean-wave spectrum and explore the mean backscatter RCS in both VV and HH channels. The theory is remarkable in its predictions for LGA scattering in that it predicts results for VV very similar to those for SPM, but in the HH channel, the mean RCS is raised substantially from its SPM value and may even be slightly higher than VV. This is much closer to observed RCS measurements. We remind the reader that we have assumed standard Gaussian surface statistics with a simple model ocean-like surface wave spectrum. No complicated hydrodynamics or shadowing has been introduced and the most important properties of our model follow from the use of a simple tangent-plane approximation.

## II. MAXWELL’S EQUATIONS VIA DYADIC GREEN’S FUNCTIONS

Suppose first that all of three-dimensional (3-D) space is divided into two regions  $\tilde{V}_1$  (the “upper region”) and  $\tilde{V}_2$  (the “lower” region) with the dividing region either a plane surface or a deformation thereof. The boundary  $\tilde{S} = \partial\tilde{V}_1$  has a unit normal  $\tilde{n}$  pointing upwards into the upper region  $\tilde{V}_1$ . Suppose further that the full dyadic Green’s functions are known for this geometry. We shall describe these shortly. Suppose further that the real atmosphere-ocean geometry is described by two regions  $V_1$  and  $V_2$  with the ocean surface at  $S = \partial V_1$ . Our goal is to make maximal use of the information about the scattering from  $\tilde{S}$  in computing scattering from the real surface  $S$ . Note that, in general, it is not necessary that the deformations relating  $\tilde{S}$ ,  $S$ , and a flat half-plane are in any sense perturbative.

$V_1$ ,  $\tilde{V}_1$  have electromagnetic properties characterized by the pair  $(\mu_1, \epsilon_1)$  and  $V_2$ ,  $\tilde{V}_2$  have EM properties characterized by the (complex) pair  $(\mu_2, \epsilon_2)$ . We assume that  $\epsilon_1 = \epsilon_0$ , the free-space electric value, and that there are no magnetic effects associated with either media so that  $\mu_1 = \mu_2 = \mu_0$ , the free-space magnetic value. Note that it is a simple matter to carry out the following analysis without these restrictions. All our fields have a time-dependence  $e^{-i\omega t}$  and the wave numbers associated with the two media are then

$$k_1 = \omega \sqrt{\epsilon_1 \mu_1}, \quad k_2 = \omega \sqrt{\epsilon_2 \mu_2}. \quad (1)$$

### A. Equations for the Background Green's Dyad

We now write down the equations characterizing the Green's dyad for the background geometry. Most of the useful existing literature on tensor or dyadic Green's functions, notably Tai [27] and Lindell [17], focuses detailed analysis on the equations for the electric Green's dyad. We shall therefore develop the theory for the electric case and take the curl of the final result to secure the magnetic field, which was developed in our PC analysis. Our initial analysis of the background geometry follows that of Tai [27]. We use superscripts 1 and 2 to denote the upper and lower medium, respectively, except on  $k$  where a subscript refers to the medium and the superscript "2" indicates a squared quantity.

Let  $\bar{r}' \in \tilde{V}_1$  and let  $\bar{r}$  be a point elsewhere in 3-D space. When  $\bar{r} \in \tilde{V}_1$ , the electric Green's dyad  $\bar{\bar{G}}_e^{11}(\bar{r}, \bar{r}')$  describing propagation of fields from  $\bar{r}'$  to  $\bar{r}$  satisfies

$$\bar{\nabla} \wedge \bar{\nabla} \wedge \bar{\bar{G}}_e^{11}(\bar{r}, \bar{r}') - k_1^2 \bar{\bar{G}}_e^{11}(\bar{r}, \bar{r}') = \bar{\bar{I}} \delta(\bar{r} - \bar{r}') \quad (2)$$

where  $\bar{\bar{I}}$  is the unit dyad. When  $\bar{r} \in \tilde{V}_2$  the dyad  $\bar{\bar{G}}_e^{21}(\bar{r}, \bar{r}')$  describing propagation of fields from  $\bar{r}'$  to  $\bar{r}$  satisfies

$$\bar{\nabla} \wedge \bar{\nabla} \wedge \bar{\bar{G}}_e^{21}(\bar{r}, \bar{r}') - k_2^2 \bar{\bar{G}}_e^{21}(\bar{r}, \bar{r}') = \bar{\bar{0}}. \quad (3)$$

These background Green's functions satisfy boundary conditions at the interface  $\tilde{S}$ . These are

$$\tilde{\bar{n}} \wedge \bar{\bar{G}}_e^{11}(\bar{r}, \bar{r}') = \tilde{\bar{n}} \wedge \bar{\bar{G}}_e^{21}(\bar{r}, \bar{r}') \quad (4)$$

$$\tilde{\bar{n}} \wedge [\bar{\nabla} \wedge \bar{\bar{G}}_e^{11}(\bar{r}, \bar{r}')] = \tilde{\bar{n}} \wedge [\bar{\nabla} \wedge \bar{\bar{G}}_e^{21}(\bar{r}, \bar{r}')]. \quad (5)$$

We now make a key hypothesis. We assume that one or both of the dyadic Green's functions defined on the regions  $\tilde{V}_1$  and  $\tilde{V}_2$  may both be uniquely continued to continuously differentiable functions as far as an open neighborhood of the real ocean-air interface  $S$ . In other words,  $\bar{\bar{G}}_e^{11}(\bar{r}, \bar{r}')$  may be continued down into the troughs—we call this a level one hypothesis—while in the corresponding level-two hypothesis, we assume, in addition, that  $\bar{\bar{G}}_e^{21}(\bar{r}, \bar{r}')$  may be continued up into the peaks and we can write down expressions involving derivatives of these objects evaluated on the real interface. It should be appreciated that the level-two hypothesis appears to be true only for lossless media—if one approaches the PC limit, the object  $\bar{\bar{G}}_e^{21}(\bar{r}, \bar{r}')$  blows up in the upper region.

### B. Electric Field Equations

The electric fields  $\bar{E}_1(\bar{r})$  and  $\bar{E}_2(\bar{r})$  in the two real regions  $V_1$  and  $V_2$  satisfy

$$\bar{\nabla} \wedge \bar{\nabla} \wedge \bar{E}_1(\bar{r}) + k_1^2 \bar{E}_1(\bar{r}) = i\omega\mu_1 \bar{J}_1(\bar{r}) \quad (6)$$

$$\bar{\nabla} \wedge \bar{\nabla} \wedge \bar{E}_2(\bar{r}) + k_2^2 \bar{E}_2(\bar{r}) = \bar{0} \quad (7)$$

where  $\bar{J}_1(\bar{r})$  is the source in  $V_1$ . They also satisfy boundary conditions on the real interface which may be written as follows:

$$\bar{n} \wedge \bar{E}_1 = \bar{n} \wedge \bar{E}_2 \quad (8)$$

$$\bar{n} \wedge \bar{\nabla} \wedge \bar{E}_1 = \bar{n} \wedge \bar{\nabla} \wedge \bar{E}_2. \quad (9)$$

These express, respectively, continuity of the tangential components of the electric and magnetic fields across the real interface, bearing in mind  $\mu_1 = \mu_2 = \mu_0$ .

By integrating the divergence of a vector field built from the Green's function and the electric field over  $V_1$  and applying the divergence theorem [27, p. 70], we obtain our first formula for the total field in region 1

$$\begin{aligned} \bar{E}_1(\bar{r}') &= i\omega\mu_1 \int_V dV \bar{J}_1(\bar{r}) \cdot \bar{\bar{G}}_e^{11}(\bar{r}, \bar{r}') \\ &+ \int_S dS \{ [\bar{n} \wedge \bar{E}_1(\bar{r})] \cdot [\bar{\nabla} \wedge \bar{\bar{G}}_e^{11}(\bar{r}, \bar{r}')] \\ &+ i\omega [\bar{n} \wedge \bar{B}_1(\bar{r})] \cdot [\bar{\bar{G}}_e^{11}(\bar{r}, \bar{r}')] \}. \end{aligned} \quad (10)$$

Here, both the volume and surface integrals are over the  $\bar{r}$ -coordinate, leading to the electric field evaluated at  $\bar{r}'$ . The corresponding integration over  $\bar{r}$  in region  $V_2$  gives the extended boundary condition

$$\begin{aligned} \bar{0} &= \int_S dS \{ [\bar{n} \wedge \bar{E}_2(\bar{r})] \cdot [\bar{\nabla} \wedge \bar{\bar{G}}_e^{21}(\bar{r}, \bar{r}')] \\ &+ i\omega [\bar{n} \wedge \bar{B}_2(\bar{r})] \cdot [\bar{\bar{G}}_e^{21}(\bar{r}, \bar{r}')] \} \end{aligned} \quad (11)$$

valid with  $\bar{r}' \in V_1$ . In both cases, the normal  $\bar{n}$  is taken to be the upward pointing normal to  $S$  (i.e., into  $V_1$ ).

Note that the volume integral gives the contribution to scattering from the geometry for which the Green's function is known and the surface integral gives corrections based on an approximate local boundary condition.

### III. DIELECTRIC GREEN'S FUNCTIONS

Several authors have given various expressions for the Green's function associated with a dielectric half-space, including Felsen and Marcuvitz [7] and Tai [27]. Between them, these authors make the point that the Green's function can be expressed in various ways and that some form of asymptotic expansion can be done. In this section, we exploit some work by Lindell [17], which gives asymptotic expressions for the reflection and transmission Green's dyads when  $S$  is a flat plane. We should warn the reader that some effort is required to map Lindell's results on to our own due to differences in conventions and various simplifications we have employed. We shall not describe the steps we have taken here in detail. Rather, we shall demonstrate that the asymptotic forms we write down satisfy the Green's function boundary conditions.

To make contact with Lindell's analysis, we choose particular coordinates and bases. We introduce Cartesian coordinates  $(x, y, z)$  with associated orthogonal unit vectors  $(\bar{u}_x, \bar{u}_y, \bar{u}_z)$  and the standard polar coordinates  $(r, \theta, \phi)$  and their associated orthogonal unit vectors  $(\bar{u}_r, \bar{u}_\theta, \bar{u}_\phi)$ . Let  $\bar{k} = \bar{k}_H + k_z \bar{u}_z$  be the outgoing wave vector.  $\bar{S}$  is taken to be the flat plane  $z = 0$  and reflected vectors are denoted by a caret so that  $\bar{v}$  becomes  $\hat{\bar{v}} = \bar{v} - 2(\bar{v} \cdot \bar{u}_z) \bar{u}_z$ . To define the electric dyadics  $\bar{\bar{G}}_e^{11}(\bar{r}, \bar{r}')$  and  $\bar{\bar{G}}_e^{21}(\bar{r}, \bar{r}')$  we must introduce the free-space Green's function defined by

$$G_0(\bar{r} - \bar{r}') = \frac{e^{ik|\bar{r} - \bar{r}'|}}{4\pi|\bar{r} - \bar{r}'|} \quad (12)$$

and the Fresnel coefficients defined by

$$R^{\text{TE}}(\psi) = \frac{\cos \psi - \sqrt{\epsilon - \sin^2 \psi}}{\cos \psi + \sqrt{\epsilon - \sin^2 \psi}} \quad (13)$$

$$R^{\text{TM}}(\psi) = \frac{-\epsilon \cos \psi + \sqrt{\epsilon - \sin^2 \psi}}{\epsilon \cos \psi + \sqrt{\epsilon - \sin^2 \psi}} \quad (14)$$

$$T^{\text{TE}}(\psi) = \frac{2 \cos \psi}{\cos \psi + \sqrt{\epsilon - \sin^2 \psi}} \quad (15)$$

$$T^{\text{TM}}(\psi) = \frac{2\sqrt{\epsilon - \sin^2 \psi}}{\epsilon \cos \psi + \sqrt{\epsilon - \sin^2 \psi}} \quad (16)$$

where  $\epsilon = \epsilon_2/\epsilon_1$  is the relative permittivity and where  $\psi$  is the local angle of incidence between an incident wave vector  $\bar{\kappa}$  and the unit normal  $\bar{n}$  to the surface so that  $\cos \psi = -(\bar{\kappa} \cdot \bar{n})/|\bar{\kappa}|$ . We also have the relationships

$$1 + R^{\text{TE}}(\psi) = T^{\text{TE}}(\psi), \quad 1 + R^{\text{TM}}(\psi) = T^{\text{TM}}(\psi) \quad (17)$$

and

$$1 - R^{\text{TE}}(\psi) = \beta T^{\text{TE}}(\psi), \quad 1 - R^{\text{TM}}(\psi) = \frac{\epsilon}{\beta} T^{\text{TM}}(\psi) \quad (18)$$

where  $\beta = \beta_2/\beta_1$  and  $\beta_i = \sqrt{k_i^2 - |\bar{k}_H|^2}$ . Note that we will just write  $R^{\text{TE}}$ ,  $R^{\text{TM}}$ ,  $T^{\text{TE}}$ , and  $T^{\text{TM}}$  for the Fresnel coefficients when considering the flat  $z = 0$  surface with  $\bar{n} = \bar{u}_z$  and  $\bar{\kappa} = -\bar{k}$ .

Using Lindell's asymptotic expression for the reflection part of the asymptotic Green's dyadic [17, p. 221] and adding in the contribution direct from the source gives the following asymptotic expression for  $\bar{G}_e^{11}(\bar{r}, \bar{r}')$ :

$$\begin{aligned} \bar{G}_e^{11}(\bar{r}, \bar{r}') \sim & \{[1 + R^{\text{TE}} e^{2ik_z \eta}] \bar{u}_\phi \bar{u}_\phi \\ & + [\bar{u}_\theta + R^{\text{TM}} e^{2ik_z \eta} \hat{\bar{u}}_\theta] \bar{u}_\theta\} G_0(\bar{r}') e^{-i\bar{k} \cdot \bar{r}} \end{aligned} \quad (19)$$

where  $\eta = \bar{r} \cdot \bar{u}_z$  is the surface height. Similarly his expression for the asymptotic form of the transmission Green's dyadic  $\bar{G}_e^{21}(\bar{r}, \bar{r}')$  can be shown to be equivalent to

$$\begin{aligned} \bar{G}_e^{21}(\bar{r}, \bar{r}') \sim & \{T^{\text{TE}} \bar{u}_\phi \bar{u}_\phi + T^{\text{TM}} \bar{u}_\theta \bar{u}_\theta + (1 - 1/\beta) \\ & \cdot \sin \theta T^{\text{TM}} \bar{u}_z \bar{u}_\theta\} G_0(\bar{r}') e^{-i\bar{k} \cdot \bar{r}} e^{ik_z(1-\beta)\eta}. \end{aligned} \quad (20)$$

To confirm that these expressions are the correct dyads for the flat dielectric plane we will check that they satisfy the boundary conditions given in (4) and (5). The first boundary condition is easily checked by taking  $\bar{n} = \bar{u}_z$  and  $\eta = 0$  and writing

$$\begin{aligned} \bar{u}_z \wedge [\bar{G}_e^{11} - \bar{G}_e^{21}] = & \{[1 + R^{\text{TE}} - T^{\text{TE}}] [\bar{u}_z \wedge \bar{u}_\phi] \bar{u}_\phi \\ & + [1 + R^{\text{TM}} - T^{\text{TM}}] [\bar{u}_z \wedge \bar{u}_\theta] \bar{u}_\theta\} G_0(\bar{r}') e^{-i\bar{k} \cdot \bar{r}} \end{aligned} \quad (21)$$

where we have used  $\bar{u}_z \wedge \bar{u}_\theta = \bar{u}_z \wedge \hat{\bar{u}}_\theta$ . Since the Fresnel coefficients satisfy (17), this is zero, as required.

The confirmation of the differential boundary condition is a little more involved as one needs to know how to find the curl of the dyads. The method of computation is described by Tai [27]. Asymptotically, for a general source point  $\bar{r}$  we have

$$\begin{aligned} \bar{\nabla} \wedge \bar{G}_e^{11}(\bar{r}, \bar{r}') \sim & ik \{[\bar{u}_\theta - R^{\text{TE}} e^{2ik_z \eta} \hat{\bar{u}}_\theta] \bar{u}_\phi \\ & - [1 - R^{\text{TM}} e^{2ik_z \eta}] \bar{u}_\phi \bar{u}_\theta\} G_0(\bar{r}') e^{-i\bar{k} \cdot \bar{r}} \end{aligned} \quad (22)$$

and

$$\begin{aligned} \bar{\nabla} \wedge \bar{G}_e^{21}(\bar{r}, \bar{r}') \sim & ik \left\{ \frac{1}{2} T^{\text{TE}} [(\bar{u}_\theta - \hat{\bar{u}}_\theta) + \beta(\hat{\bar{u}}_\theta + \bar{u}_\theta)] \bar{u}_\phi \right. \\ & \left. - \frac{\epsilon}{\beta} T^{\text{TM}} \bar{u}_\phi \bar{u}_\theta \right\} G_0(\bar{r}') e^{-i\bar{k} \cdot \bar{r}} e^{ik_z(1-\beta)\eta}. \end{aligned} \quad (23)$$

Hence, placing  $\bar{r}$  on the flat plane, we get, asymptotically

$$\begin{aligned} \bar{u}_z \wedge \{\bar{\nabla} \wedge [\bar{G}_e^{11}(\bar{r}, \bar{r}') - \bar{G}_e^{21}(\bar{r}, \bar{r}')]\} \\ = ik \left\{ ([1 - R^{\text{TE}}] - \beta T^{\text{TE}}) \bar{u}_z \wedge \bar{u}_\theta \right. \\ \left. - \left( [1 - R^{\text{TM}}] - \frac{\epsilon}{\beta} T^{\text{TM}} \right) \bar{u}_z \wedge \bar{u}_\phi \right\} G_0(\bar{r}') e^{-i\bar{k} \cdot \bar{r}}. \end{aligned} \quad (24)$$

But since the Fresnel coefficients satisfy (18), this is zero, as required.

#### IV. THE ROOT RCS AS A FUNCTION OF THE SURFACE FIELDS

In this section, we look at the properties of the root RCS as an integral mapping from assumed surface fields. To obtain the root RCS we use (10) for the electric field. For nonnormal backscatter, we may ignore the volume integral when the background geometry is flat. The surface integral for the magnetic field can be written down by taking the curl with respect to the primed variable

$$\begin{aligned} \bar{B}_1(\bar{r}') = & \frac{1}{i\omega} \int_S dS \{[\bar{\nabla}' \wedge \bar{F}(\bar{r}, \bar{r}')] \cdot [\bar{n} \wedge \bar{E}_1(\bar{r})] \\ & + i\omega [\bar{\nabla}' \wedge \bar{M}(\bar{r}, \bar{r}')] \cdot [\bar{n} \wedge \bar{B}_1(\bar{r})]\} \end{aligned} \quad (25)$$

where  $\bar{F}(\bar{r}, \bar{r}') = [\bar{\nabla} \wedge \bar{G}_e^{11}(\bar{r}, \bar{r}')]^T$  and  $\bar{M}(\bar{r}, \bar{r}') = [\bar{G}_e^{11}(\bar{r}, \bar{r}')]^T$ . It is then a simple matter to show that

$$\begin{aligned} \bar{\nabla}' \wedge \bar{M}(\bar{r}, \bar{r}') \sim & -ik G_0(\bar{r}') e^{-i\bar{k} \cdot \bar{r}} \{[1 + e^{2ik_z \eta} R^{\text{TE}}] \bar{u}_\theta \bar{u}_\phi \\ & + \bar{u}_\phi [\bar{u}_\theta + e^{2ik_z \eta} R^{\text{TM}} \hat{\bar{u}}_\theta]\} \end{aligned} \quad (26)$$

and

$$\begin{aligned} \bar{\nabla}' \wedge \bar{F}(\bar{r}, \bar{r}') \sim & k^2 G_0(\bar{r}') e^{-i\bar{k} \cdot \bar{r}} \{[1 - e^{2ik_z \eta} R^{\text{TM}}] \bar{u}_\phi \bar{u}_\phi \\ & + \bar{u}_\theta [\bar{u}_\theta - e^{2ik_z \eta} R^{\text{TE}} \hat{\bar{u}}_\theta]\}. \end{aligned} \quad (27)$$

With the root RCS  $\bar{\Sigma}$  defined by

$$\bar{B}_1(\bar{r}') = G_0(\bar{r}') \bar{\Sigma} + O(|\bar{r}'|^{-2}) \quad (28)$$

we can now write down the following formula where, as usual,  $c = 1/\sqrt{\mu_0 \epsilon_0}$  is the speed of light in vacuum

$$\begin{aligned} \bar{\Sigma} = & ik \int_S dS e^{-i\bar{k} \cdot \bar{r}} \{(\bar{u}_\phi \bar{\gamma} - \bar{u}_\theta \bar{\alpha}) \cdot [\bar{n} \wedge \bar{E}_1(\bar{r})] / c \\ & + (\bar{u}_\phi \bar{\delta} - \bar{u}_\theta \bar{\beta}) \cdot [\bar{n} \wedge \bar{B}_1(\bar{r})]\} \end{aligned} \quad (29)$$

where the kernels are given by  $\bar{\alpha} = (\bar{u}_\theta - e^{2ik_z \eta} R^{\text{TE}} \hat{\bar{u}}_\theta)$ ,  $\bar{\beta} = (1 + e^{2ik_z \eta} R^{\text{TE}}) \bar{u}_\phi$ ,  $\bar{\gamma} = -(1 - e^{2ik_z \eta} R^{\text{TM}}) \bar{u}_\phi$ , and  $\bar{\delta} = (\bar{u}_\theta + e^{2ik_z \eta} R^{\text{TM}} \hat{\bar{u}}_\theta)$ . To obtain the polarization components of the root RCS, we take the scalar product of (29) with  $-\bar{u}_\theta$  and  $\bar{u}_\phi$ , respectively. We let  $\Sigma(*H)$  denote the root RCS for

H receive and either transmitted polarization and  $\Sigma(*V)$  is the corresponding root RCS for V- receive. Then

$$\Sigma(*H) = ik \int dS e^{-i\bar{k} \cdot \bar{r}} \{ \bar{\alpha} \cdot (\bar{n} \wedge \bar{E})/c + \bar{\beta} \cdot (\bar{n} \wedge \bar{B}) \} \quad (30)$$

$$\Sigma(*V) = ik \int dS e^{-i\bar{k} \cdot \bar{r}} \{ \bar{\gamma} \cdot (\bar{n} \wedge \bar{E})/c + \bar{\delta} \cdot (\bar{n} \wedge \bar{B}) \}. \quad (31)$$

Note that at this stage we have made *no* assumptions about the nature of the surface fields, so our result may be viewed as a mapping from surface fields to cross sections with several interesting properties. The reader may notice that the vectors  $\bar{\alpha}, \bar{\beta}, \bar{\gamma}, \bar{\delta}$  are in fact the H and V components of the electric and magnetic fields of a plane wave being scattered by a dielectric half-space. This is no coincidence and is one example of a general link between the Green's function approach and other methods recently discovered by Tough and Ward [30].

## V. EXPRESSIONS FOR THE SURFACE FIELDS

It is possible to consider three types of expression for the surface fields. These are based on: 1) the tangent-plane approximation, which is equivalent to a Leontovich-type impedance assumption; 2) a curvature-corrected impedance approximation; and 3) an extended boundary condition. Here we consider only 1). The detailed results arising from choice 2) will be considered elsewhere [24]. The implications of 3) will be discussed later.

In the tangent plane approximation for the surface fields it is assumed that each infinitesimal piece of the scattering surface  $S$  can be treated as part of an infinite dielectric plane whose normal is defined by the local normal  $\bar{n}$ . Let  $\bar{k}$  be the incident wave vector and let  $\bar{E}_i$  and  $\bar{B}_i$  incident electric and magnetic fields, respectively. The equations for the surface fields are then

$$\bar{n} \wedge \bar{E}_1 = [1 + R^{\text{TM}}(\psi)] \bar{n} \wedge \bar{E}_i - \frac{[R^{\text{TE}}(\psi) - R^{\text{TM}}(\psi)]}{|\bar{n} \wedge \bar{k}|^2} \cdot \bar{n} \cdot (\bar{n} \wedge \bar{E}_i) [\bar{k} - (\bar{n} \cdot \bar{k}) \bar{n}] \quad (32)$$

$$\bar{n} \wedge \bar{B}_1 = [1 - R^{\text{TE}}(\psi)] \bar{n} \wedge \bar{B}_i - \frac{[R^{\text{TE}}(\psi) - R^{\text{TM}}(\psi)]}{|\bar{n} \wedge \bar{k}|^2} \cdot \bar{n} \cdot (\bar{n} \wedge \bar{B}_i) [\bar{k} - (\bar{n} \cdot \bar{k}) \bar{n}]. \quad (33)$$

## VI. THE ROOT RCS IN THE TANGENT PLANE APPROXIMATION

From here we make the explicit specialization to backscatter, so that  $\bar{k} = -\bar{k} = k_1 \bar{u}_r$ . For transmitted horizontal polarization, we have an incoming wave of the form

$$\bar{E}_i = -E_0 \bar{u}_\phi e^{-i\bar{k} \cdot \bar{r}}, \quad \bar{B}_i = -B_0 \bar{u}_\theta e^{-i\bar{k} \cdot \bar{r}}. \quad (34)$$

For transmitted vertical polarization, we have an incoming wave of the form

$$\bar{E}_i = -E_0 \bar{u}_\theta e^{-i\bar{k} \cdot \bar{r}}, \quad \bar{B}_i = B_0 \bar{u}_\phi e^{-i\bar{k} \cdot \bar{r}}. \quad (35)$$

In these relations,  $E_0 = cB_0$ .

As a preliminary to working out all the terms in our integrands, we substitute each of these expressions for the incoming fields into (32) and (33), and then take the dot products of the resulting expressions with our basis vectors, and use some vector identities to simplify the results. Substituting

the resulting relations into our expressions for the horizontal and vertical polarization root RCS and dividing by  $B_0$  gives us the scattered field per unit in field (the root RCS proper). To state our results in a compact form we now introduce some polarization functions defined by

$$\Theta(HH) = -1, \quad \Theta(VV) = +1 \quad (36)$$

$$R(HH) = R^{\text{TE}}, \quad R(VV) = -R^{\text{TM}} \quad (37)$$

$$P(HH) = R^{\text{TE}}(\psi), \quad P(VV) = -R^{\text{TM}}(\psi). \quad (38)$$

The root RCS can then be written

$$\Sigma(\text{pol}) = i \int dS e^{-2i\bar{k}_H \cdot \bar{x} - 2ik_z \eta} \mathcal{K}(\text{pol}) + i\Theta(\text{pol})R(\text{pol}) \int dS e^{-2i\bar{k}_H \cdot \bar{x}} \mathcal{H}(\text{pol}) \quad (39)$$

where, in the integrands,  $\mathcal{K}(\text{pol})$  denotes the dielectric Kirchhoff component and  $\mathcal{H}(\text{pol})$  denotes the half-space Green's function corrections. The Kirchhoff components are given by

$$\mathcal{K}(\text{pol}) = (\bar{n} \cdot \bar{k}) \left\{ [R^{\text{TM}}(\psi) + R^{\text{TE}}(\psi)] - \Theta(\text{pol})k^2 \cdot \frac{[R^{\text{TE}}(\psi) - R^{\text{TM}}(\psi)]}{|\bar{n} \wedge \bar{k}|^2} [(\bar{n} \cdot \bar{u}_\theta)^2 - (\bar{n} \cdot \bar{u}_\phi)^2] \right\}. \quad (40)$$

Note that this contribution is itself polarization sensitive.

The half-space corrections are given by

$$\mathcal{H}(\text{pol}) = \bar{n} \cdot (\bar{k} - \hat{\bar{k}}) - P(\text{pol}) \bar{n} \cdot (\bar{k} + \hat{\bar{k}}) + (\bar{n} \cdot \bar{k}) \cdot \left\{ \cos 2\theta [R^{\text{TM}}(\psi) - R^{\text{TE}}(\psi)] + k^2 \cdot \frac{[R^{\text{TE}}(\psi) - R^{\text{TM}}(\psi)]}{|\bar{n} \wedge \bar{k}|^2} [\cos 2\theta (\bar{n} \cdot \bar{u}_\theta)^2 + (\bar{n} \cdot \bar{u}_\phi)^2] \right\}. \quad (41)$$

We now have the root RCS for VV and HH as explicit, if very complicated, functions of the local height and normal. We can now, at least in principle, take the modulus squared of these expressions and average over the joint distribution of heights and slopes.

## VII. THE LSV METHOD OF APPROXIMATION

In the previous section, we wrote down various integrals for the root RCS. The problem is, therefore, to evaluate them. To do this we note that since the integrands are functionals of the surface height and slope, we can expand them up to any order in the slopes. One can then attempt to evaluate the resulting integrals order by order. When this expansion is carried out up to linear order about the flat case, we say we have an LSV approximation to the root RCS. Similarly, if this is carried out up to quadratic order, we call this a QSV approximation. These approximations are, therefore, valid when the surface slopes are small. An issue arises as to what other values of the slope could be used as the base point of the expansion. In his pioneering analysis of dielectrics, Hagfors [9] considered making an expansion about that slope that results in specular reflection. In our own studies we considered this in some detail, but discarded this approach as 1) the relationship to

SPM of the resulting model is very awkward and 2) such a specular point may not exist for LGA incidence or may be shadowed. In what follows, we will only consider the LSV approximation, though it is possible to give extensions to QSV or to a Hagfors-style approximation.

Let  $\eta_x = \partial\eta/\partial x$  and  $\eta_y = \partial\eta/\partial y$  so that  $\bar{n} = T^{-1}(-\eta_x, -\eta_y, 1)$  and  $dS = T dx dy$  where  $T = [1 + \eta_x^2 + \eta_y^2]^{1/2}$ . Furthermore, with conventions that the wave is incident from the right at an angle  $\theta$  from normal, we have  $\bar{k} = k(\sin \theta, 0, \cos \theta)$ ,  $\bar{u}_\phi = (0, 1, 0)$  and  $\bar{u}_\theta = (\cos \theta, 0, -\sin \theta)$ . In this approximation, we expand all integrals about  $(\eta_x, \eta_y) = (0, 0)$ . We have the following exact relations:

$$dS(\bar{n} \cdot \bar{k}) = d^2 \bar{x} k (\cos \theta - \eta_x \sin \theta) \quad (42)$$

$$dS(\bar{n} \cdot \hat{\bar{k}}) = -d^2 \bar{x} k (\cos \theta + \eta_x \sin \theta) \quad (43)$$

and the expansions denoting by  $*$  either  $\eta_x$  or  $\eta_y$

$$\begin{aligned} \bar{n} \cdot \bar{u}_\theta &= -T^{-1}(\sin \theta + \eta_x \cos \theta) \\ &= -(\sin \theta + \eta_x \cos \theta) + O(*^2) \end{aligned} \quad (44)$$

$$\bar{n} \cdot \bar{u}_\phi = -T^{-1} \eta_y = -\eta_y + O(*^2) \quad (45)$$

$$\frac{k^2}{|\bar{n} \wedge \bar{k}|^2} (\bar{n} \cdot \bar{u}_\theta)^2 = 1 + O(*^2). \quad (46)$$

The local reflection coefficients can be expanded about their flat space values as follows:

$$R^{\text{TE}}(\psi) = R^{\text{TE}} + R_1^{\text{TE}} \eta_x + O(*^2) \quad (47)$$

$$R^{\text{TM}}(\psi) = R^{\text{TM}} + R_1^{\text{TM}} \eta_x + O(*^2). \quad (48)$$

The reflection coefficient linear deviation functions are given by

$$R_1^{\text{TE}} = \frac{2(1-\epsilon) \sin \theta}{\sqrt{\epsilon - \sin^2 \theta} (\cos \theta + \sqrt{\epsilon - \sin^2 \theta})^2} \quad (49)$$

$$R_1^{\text{TM}} = \frac{-2\epsilon(1-\epsilon) \sin \theta}{\sqrt{\epsilon - \sin^2 \theta} (\epsilon \cos \theta + \sqrt{\epsilon - \sin^2 \theta})^2}. \quad (50)$$

Define the polarization function  $R_1(\text{pol})$  by

$$R_1(HH) = R_1^{\text{TE}}, \quad R_1(VV) = -R_1^{\text{TM}}. \quad (51)$$

The expansions to linear order for the integrands can then be written

$$\begin{aligned} dS\mathcal{K}(\text{pol}) &= -2d^2 \bar{x} k \Theta(\text{pol}) \{ [R(\text{pol}) \cos \theta \\ &\quad + [R_1(\text{pol}) \cos \theta - R(\text{pol}) \sin \theta] \eta_x] + O(*^2) \end{aligned} \quad (52)$$

and

$$dS\mathcal{H}(\text{pol}) = 2d^2 \bar{x} k [\cos \theta + R(\text{pol}) \sin \theta \eta_x] + O(*^2). \quad (53)$$

Noting that integration by parts implies

$$\int d^2 \bar{x} e^{-i\bar{k}_H \cdot \bar{x} - ik_z \eta} \eta_x = -\frac{k_H}{k_z} C(\bar{k}_H, k_z) \quad (54)$$

$$\int d^2 \bar{x} e^{-i\bar{k}_H \cdot \bar{x}} \eta_x = ik_H D(\bar{k}_H) \quad (55)$$

where

$$C(\bar{k}_H, k_z) = \int d^2 \bar{x} e^{-i\bar{k}_H \cdot \bar{x} - ik_z \eta} \quad (56)$$

$$D(\bar{k}_H) = \int d^2 \bar{x} e^{-i\bar{k}_H \cdot \bar{x}} \eta \quad (57)$$

it is then straight forward to show that ignoring a delta function that contributes only at normal incidence, we have the following expression for the root RCS:

$$\begin{aligned} \Sigma(\text{pol}) &= -2i\Theta(\text{pol}) \left\{ \left[ \frac{k^2}{k_z} R(\text{pol}) - k \sin \theta R_1(\text{pol}) \right] \right. \\ &\quad \left. \cdot C(2\bar{k}_H, 2k_z) - 2ik^2 \sin^2 \theta R^2(\text{pol}) D(2\bar{k}_H) \right\}. \end{aligned} \quad (58)$$

This expression for the root RCS reduces to the PC result, given by (64) of [21], as the conductivity becomes infinite.

### VIII. AGREEMENT WITH SPM

The relationship of the LSV half-space model to SPM is easy to explore, as we have treated the analysis of the dielectric formula quasi-perturbatively. The height is modeled exactly, but the slopes are treated perturbatively for the purpose only of modeling the variation of the reflection coefficients.

Valenzuela's perturbation result [31] for the root RCS may be written

$$\begin{aligned} \Sigma^{\text{val}}(\text{pol}) &= -4\Theta(\text{pol}) k^2 \{ R(\text{pol}) \cos^2 \theta \\ &\quad - A(\text{pol}) \sin^2 \theta \} D(2\bar{k}_H) \end{aligned} \quad (59)$$

where  $A(HH) = 0$  and  $A(VV) = -(1/2)[1 - \epsilon^{-1}](1 - R^{\text{TM}})^2$ . The SPM limit of our model is given by making the expansion  $C(2\bar{k}_H, 2k_z) \sim (2\pi)^2 \delta(2\bar{k}_H) - 2ik_z D(2\bar{k}_H)$ . Ignoring the delta function as usual (as we are not considering almost normal incidence) we obtain

$$\begin{aligned} \Sigma(\text{pol}) &= -4k^2 \Theta(\text{pol}) \{ R(\text{pol}) [1 + R(\text{pol}) \sin^2 \theta \\ &\quad - \sin \theta \cos \theta R_1(\text{pol})] \} D(2\bar{k}_H). \end{aligned} \quad (60)$$

These are clearly not the same. To see by how much they differ, we can expand Valenzuela's results and our own in inverse powers of  $N = \sqrt{\epsilon}$ . This gives us

$$\Sigma^{\text{val}}(HH) \sim -4k^2 (1 - \sin^2 \theta) [1 - 2 \cos \theta N^{-1} \\ + 2 \cos^2 \theta N^{-2}] + O(N^{-3}) \quad (61)$$

$$\begin{aligned} \Sigma^{\text{val}}(VV) &\sim -4k^2 [(1 + \sin^2 \theta) [1 - 2 \sec \theta N^{-1} \\ &\quad + (2 \sec^2 \theta)(1 + 2 \sin^2 \theta \\ &\quad - \sin^2 \theta \cos^2 \theta) N^{-2}] + O(N^{-3}) \end{aligned} \quad (62)$$

and

$$\begin{aligned} \Sigma(HH) &\sim -4k^2 (1 - \sin^2 \theta) [1 - 2 \cos \theta N^{-1} \\ &\quad + 2(\cos^2 \theta - \sin^2 \theta) N^{-2}] + O(N^{-3}) \end{aligned} \quad (63)$$

$$\begin{aligned} \Sigma(VV) &\sim -4k^2 [(1 + \sin^2 \theta) [1 - 2 \sec \theta N^{-1} \\ &\quad + (2 \sec^2 \theta)(1 + 2 \sin^2 \theta) N^{-2}] + O(N^{-3}) \end{aligned} \quad (64)$$

Comparison of the exact SPM results with the results from the LSV model therefore yield agreement at  $O(N^0)$  (perfectly conducting) and at  $O(N^{-1})$ , but not at  $O(N^{-2})$ .

We remind the reader that the preceding analysis assumes a tangent plane approximation for the surface fields. This, at  $O(N^{-1})$ , is consistent with imposing a Leontovich-type

impedance boundary condition. It can be shown [24] that inclusion of first-order curvature corrections improves agreement with SPM to  $O(N^{-2})$ . Better still, if we impose an extended boundary condition it can also be shown that the agreement with SPM is *exact*. However, in this case, the model can be only used for near lossless materials due to the failure of the level two continuation hypothesis for conducting media. The model presented here is really to be regarded as a model for “high-contrast” media, where  $|N|$  is large.

## IX. RCS FOR A STATISTICAL SURFACE

If we take our expression for the root RCS, take expectations of its modulus, and normalize the result, we obtain the following expression for the mean RCS per unit area

$$\langle \sigma \rangle = 16\pi k^4 \left[ |E(\text{pol})|^2 \frac{e^{-4k_z^2 s^2}}{4k_z^2} \Phi(2\bar{k}_H, 2k_z) + (2\text{Re}\{[E(\text{pol})][R^2(\text{pol})]^*\}) e^{-2k_z^2 s^2} \sin^2 \theta + |R^2(\text{pol})|^2 \sin^4 \theta \Psi^S(2\bar{k}_H) \right] \quad (65)$$

where  $E(\text{pol}) = R(\text{pol}) - (1/2) \sin 2\theta R_1(\text{pol})$ , the Kirchhoff integral  $\Phi(\bar{k}_H, k_z)$ , is defined by

$$\Phi(\bar{k}_H, k_z) = \frac{1}{(2\pi)^2} \int d^2\bar{x} e^{-i\bar{k}_H \cdot \bar{x}} \{ \exp[k_z^2 W(\bar{x})] - 1 \} \quad (66)$$

the correlation function  $W(\bar{x})$  is defined by

$$W(\bar{x}) = \int d^2\bar{k} e^{i\bar{k} \cdot \bar{x}} \Psi^S(\bar{k}). \quad (67)$$

$s^2 = W(\bar{0})$  is the mean square wave height,  $\Psi^S(\bar{k}) = (1/2)[\Psi(\bar{k}) + \Psi(-\bar{k})]$ , and  $\Psi(\bar{k})$  is the surface wave spectrum. The formula given in (65) is, as far as we aware, the first to combine elements of Kirchhoff theory, the properties of a dielectric, and multiple scattering effects.

This model contains several previous models as limiting cases. For small  $\theta$ , it gives the Holliday model [10] with dielectric corrections. As the relative dielectric constant becomes infinite it approaches our previous half-space perfectly conducting model as expressed by [21, eq. (70)]; that model itself reduced to the perfectly conducting SPM model exactly in the limit of very small surface height. We have already demonstrated that this agreement with SPM has been extended to high-contrast dielectrics.

## X. PROPERTIES OF THE RCS

Although our formulas can only be evaluated (with present machinery) to low order in the slope variations, it is well worth looking at what they predict. Even the low-order results indicate interesting new features compared to the perfectly conducting model and to perturbation theory. We are here concerned mainly with the ocean surface, but our result (65) for the mean backscatter RCS may in principle be used for any Gaussian surface bounding a high-contrast medium where the surface is characterized by a spectrum. Here we shall investigate the RCS based on a simple model spectrum for the ocean background where the Kirchhoff integral can

be done essentially exactly in closed form. It can be also be applied to more realistic spectra such as the detailed spectrum presented by Apel [1] and to the radar imagery in the same way as was carried out by Holliday [10], based on modulations of the surface-wave spectrum. Note that we disagree with both these authors in several respects. Not only have we changed the mapping from the spectrum to the RCS to account for dielectric effects and limited multiple scattering, but we also believe that the traditional specular limit model for near-normal incidence (used by both authors) is invalid (as discussed in [23]). Here we shall confine ourselves to incidence angles well away from normal, so that at least for our model spectrum, the results of [22] for the Kirchhoff integral may be used. This is an simple and accurate analytic model that replaces the detailed numerics of [10].

We shall consider two issues. First, we present some plots to show the influence of dielectric properties compared to perfect conductivity. Then, we look at varying the wind speed. We use a model spectrum

$$\Psi(\bar{k}) = \begin{cases} \frac{b}{\pi} k^{-4} \exp(-k_0/k), & \text{if } \bar{k} \cdot \bar{u} \geq 0 \\ 0, & \text{otherwise} \end{cases} \quad (68)$$

where  $\bar{u}$  is the steady wind velocity,  $k_0$  is of order  $g/u^2$ , and  $b$  is a parameter determined empirically. This is identical to that discussed in [10], [21] and we use all the asymptotic machinery developed for evaluating the statistical Kirchhoff integral  $\Phi$  given in [22] and [23].

### A. The Influence of Imperfect Conductivity

In this section, we present some plots to show, for various scattering models, the influence of finite conductivity versus perfect conductivity. We explore this for two scattering models, Valenzuela's SPM model and the half-space model in LSV approximation. In each case, we consider two values of the conductivity, labeled “typical” and “large.” The “typical” refers to sea water, which has a conductivity of 4 S/m and a relative dielectric constant of 81 (values from Ishimaru [13]). The “large” refers to a conductivity of 40 000 S/m and the same dielectric constant. The complex dielectric constants considered are, therefore, given by  $\epsilon = 81 + i(56.4, 564 000)$ . In this series of examples, we work at L-Band with a wind-speed of 2 m/s.

We see that whatever the model, there is very little influence of the conductivity on the HH cross-section behavior. However, the VV values are significantly different in the LGA domain. The plots demonstrate the singular nature of the LGA/high conductivity limits. For finite conductivity, there is a gentle decline in the VV amplitude as we approach grazing, which is not the case in the PC limit. The effect of finite conductivity is to significantly depress the VV RCS in the LGA domain, compared to its PC value. This is independent of the scattering model.

The SPM HH values are much lower than the half-space values. This was also true in the PC case and will be explored further in the next subsection.

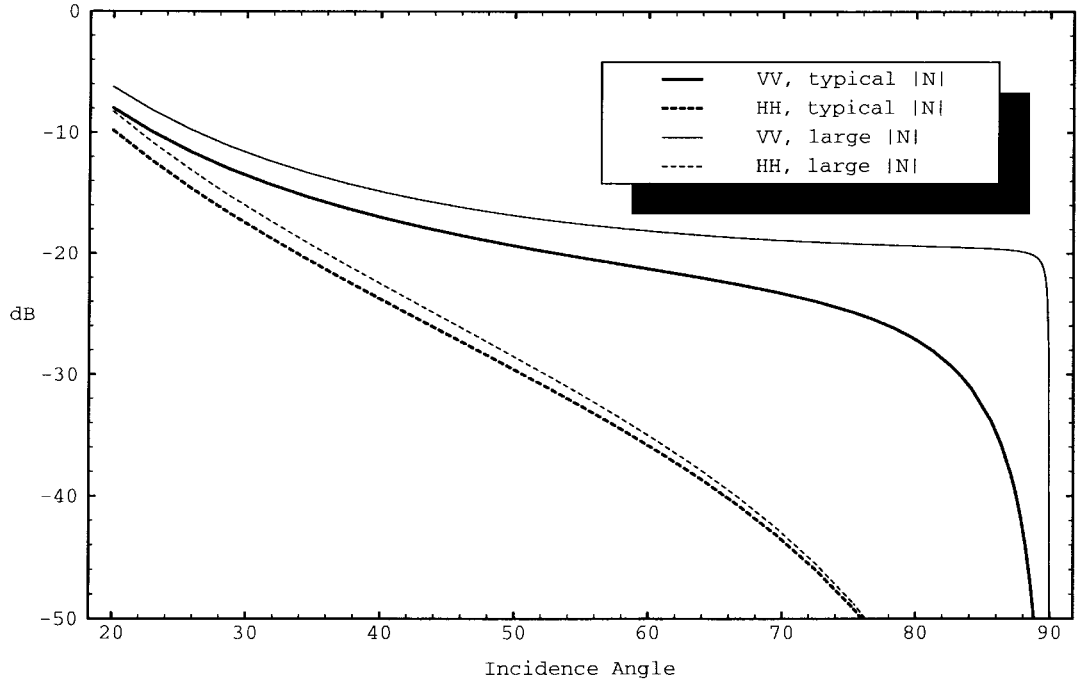


Fig. 1. SPM cross sections for various conductivities.

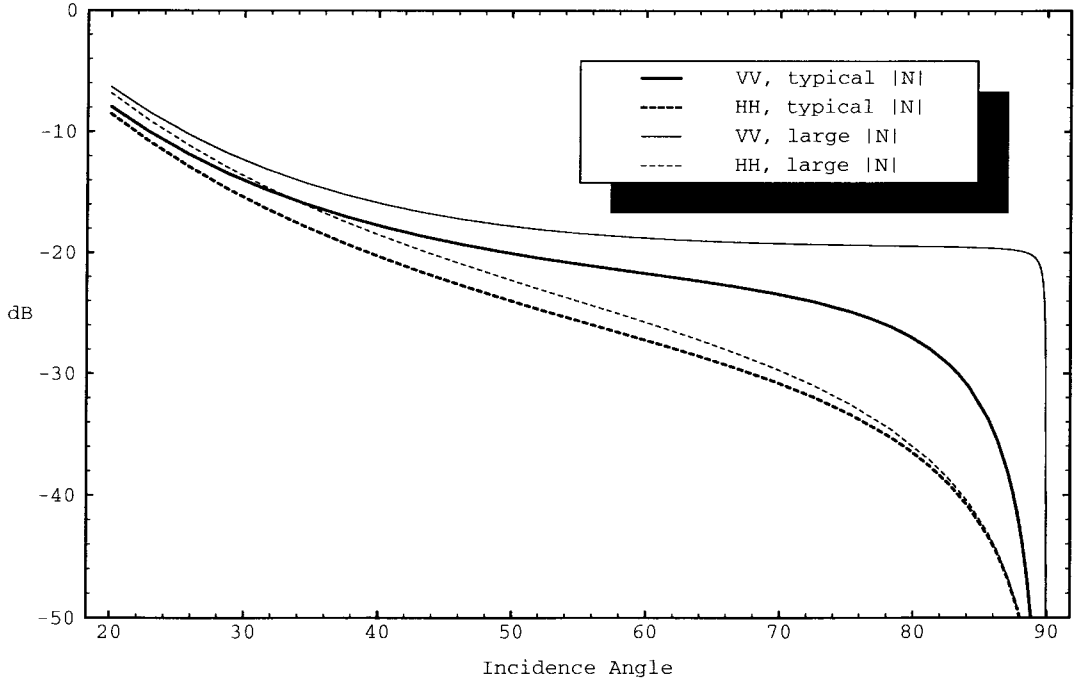


Fig. 2. Half-space cross sections for various conductivities.

### B. SPM Versus Half-Space and Influence of Wind Speed

The next two diagrams explore the relationship between SPM and the half-space model for two different wind speeds. The results may be summarized easily enough. The half-space model in the LSV approximation tracks the SPM result quite closely in the VV channel, but gives significantly higher results in HH. As the wind speed increases, the HH RCS grows and can be higher than VV. Note that we are only working in the LSV approximation—we might expect further corrections

from the QSV variant to become important as the wind speed grows still further. What is important is that the half-space model only reduces to the SPM limit for tiny mean square wave heights—for applications of any practical relevance at L-band or higher frequencies, SPM is not relevant.

It is noteworthy that these plots, at least for lower wind speed, suggest that this model is a significant improvement over other existing models in explaining the observed RCS levels. Apel [1] noted that satisfactory agreement with data

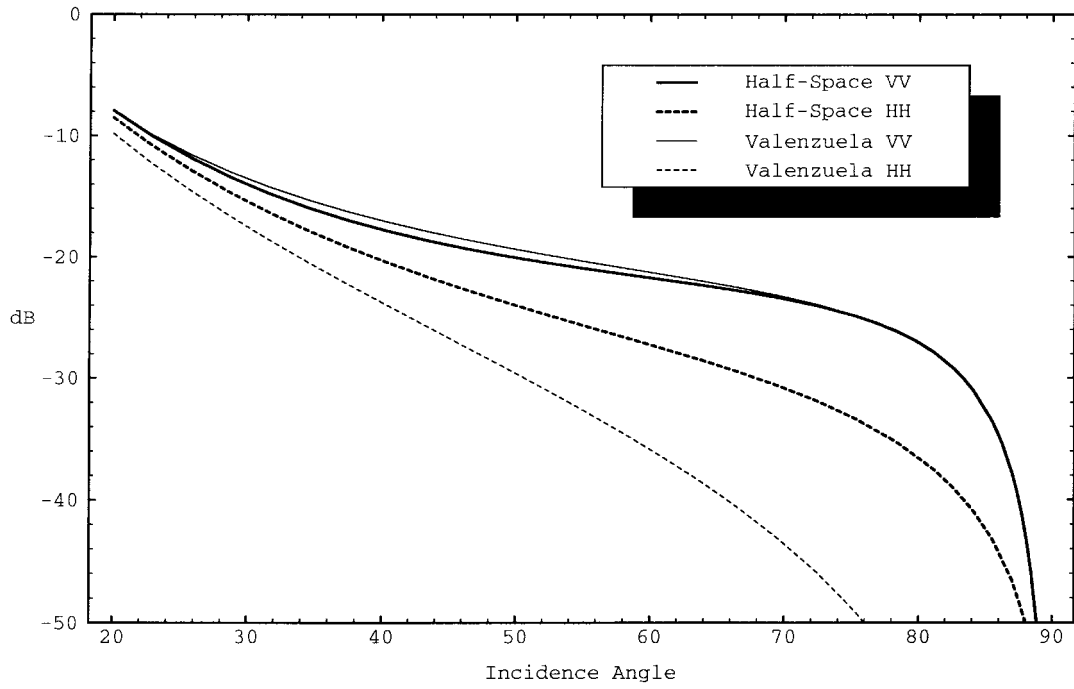


Fig. 3. Half-space versus SPM for low wind speed.

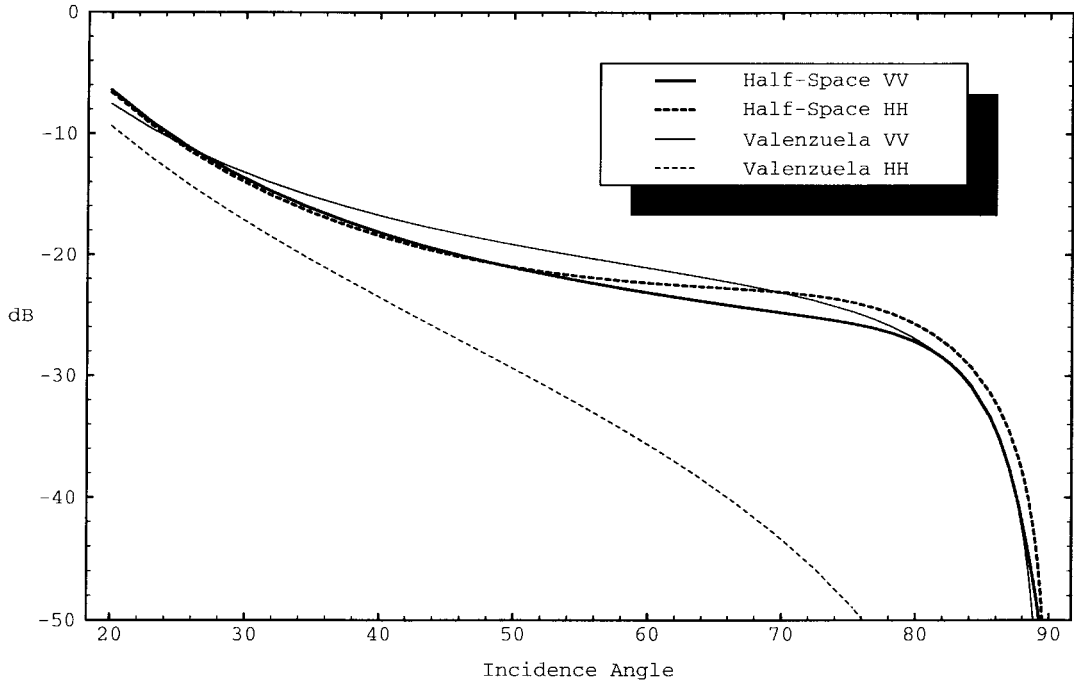


Fig. 4. Half-space versus SPM for intermediate wind speed.

could be obtained in VV using SPM, but that the SPM HH levels were much too low. The present model dramatically elevates the HH levels. We might argue that this preliminary dielectric model resolves the single biggest issue raised by Apel—that of the gross levels of the VV and HH cross sections.

The other “unexplained features” mentioned in our introduction deserve comment. We have extended this model

to time-dependent phenomena and analyzed Doppler spectra with encouraging results; details will be given elsewhere. The associated question of “spikes” is more mysterious. It should be appreciated that most statistical models of the general type presented here only address the question of calculating the mean backscatter RCS. The likelihood of sporadic larger values is not addressed since we have calculated neither the probability distribution of the RCS nor associated measures of

spread such as the variance. It is not so much that the question has not been answered; rather the question of the likelihood of spikes has not been posed within this framework.

## XI. CONCLUSIONS

In this paper, we have shown how refinement of the Green's function can be combined with approximate boundary conditions to produce a tractable model of the RCS and mean backscatter RCS for statistical surfaces that are the boundary of a high-contrast dielectric medium. For LGA backscatter from ocean-like surfaces, the model predicts VV returns similar to those predicted from first-order perturbation theory, but HH returns that are significantly higher than those predicted by SPM. This prediction has been obtained through a simple refinement of the Green's function, representing a simple electromagnetic modification to an otherwise familiar type of theory with Gaussian surface statistics, a simple model ocean-like surface wave spectrum, and no complex hydrodynamics or shadowing.

The theory we have presented reduces to a pure dielectric Kirchhoff model for near-normal incidence and to Holliday *et al.* ocean-scattering model [10] for simultaneous near-normal incidence and perfect conductivity. For very small surface heights, it reduces to Valenzuela's SPM model [31] for dielectrics with a large refractive index.

The theory presented here is capable of considerable further development and we intend to continue the program of refining the Green's function and to consider variant boundary conditions with and without shadowing.

## ACKNOWLEDGMENT

The authors would like to thank A. Jolly, T. Lamont-Smith, B. C. Barber, R. J. A. Tough, and K. D. Ward for helpful discussions.

## REFERENCES

- [1] J. R. Apel, "An improved model of the ocean surface wave vector spectrum and its effect on radar backscatter," *J. Geophys. Res.*, vol. 99, p. 18269, Aug. 1994.
- [2] D. H. Berman and J. S. Perkins, "The Kirchhoff approximation and first-order perturbation theory for rough surface scattering," *J. Acoust. Soc. Amer.*, vol. 78, p. 1045, Sept. 1985.
- [3] G. Brown, "The validity of shadowing corrections in rough surface scattering," *Radio Sci.*, vol. 19, no. 6, p. 1461, Nov./Dec. 1984.
- [4] G. S. Brown, "Backscattering from a Gaussian-distributed perfectly conducting rough surface," *IEEE Trans. Antennas Propagat.*, vol. AP-26, p. 472, May 1978.
- [5] M. L. Burrows, "A reformulated boundary perturbation theory in electromagnetism and its application to a sphere," *Can. J. Phys.*, vol. 45, p. 1729, May 1967.
- [6] J. A. DeSanto, "Green's function for the electromagnetic scattering from a random rough surface," *J. Math. Phys.*, vol. 15, no. 3, p. 283, Mar. 1974.
- [7] L. B. Felsen and N. Marcuvitz, *Radiation and Scattering of Waves*. New York/Oxford: IEEE/OUP Press, 1994.
- [8] C. Flammer, "Variational formulae for domain functionals in electromagnetic theory," SRI Tech. Rep., 1957.
- [9] T. Hagfors, "Scattering and transmission of electromagnetic waves at a statistically rough boundary between two dielectric media," in *Electromagnetic Wave Theory*, J. Brown, Ed. Oxford: Pergamon, 1967, vol. 2, p. 997.
- [10] D. Holliday, G. St.-Cyr, and N. Woods, "A radar ocean imaging model for small to moderate incidence angles," *Int. J. Remote Sensing*, vol. 7, p. 1809, Dec. 1986.
- [11] D. Holliday, L. L. DeRaad, Jr., and G. J. St.-Cyr, "Volterra approximation for low grazing angle shadowing on smooth ocean-like surfaces," *IEEE Trans. Antennas Propagat.*, vol. 43, p. 1199, Nov. 1995.
- [12] ———, "Forward-backward: A new method for computing low-grazing angle scattering," *IEEE Trans. Antennas Propagat.*, vol. 44, p. 722, May 1996.
- [13] A. Ishimaru, *Electromagnetic Wave Propagation, Radiation, and Scattering*. Englewood Cliffs, NJ: Prentice-Hall, 1991.
- [14] D. A. Kapp and G. S. Brown, "A new numerical method for rough-surface scattering calculations," *IEEE Trans. Antennas Propagat.*, vol. 44, p. 711, May 1996.
- [15] M.-J. Kim and A. J. Stoddart, "The region of validity of perturbation theory," *Waves Random Media*, vol. 3, no. 4, p. 325, Oct. 1993.
- [16] P. H. Y. Lee, J. D. Barter, K. L. Beach, C. L. Hindman, B. M. Lake, H. Rungaldier, J. C. Shelton, A. B. Williams, R. Yee, and H. C. Yuen, "X-band microwave backscattering from ocean waves," *J. Geophys. Res.*, vol. 100, p. 2591, Feb. 1995.
- [17] I. V. Lindell, *Methods for Electromagnetic Field Analysis*. New York: IEEE/OUP Press, 1995.
- [18] K. M. Mitzner, "Effect of small irregularities on electromagnetic scattering from an interface of arbitrary shape," *J. Math. Phys.*, vol. 5, no. 12, p. 1776, Dec. 1964.
- [19] S. Mudaliar, "Green's function of a randomly rough surface," *Can. J. Phys.*, vol. 72, no. 1-2, p. 20, Jan./Feb. 1994.
- [20] M. I. Sancer, "Shadow-corrected electromagnetic scattering from a randomly rough surface," *IEEE Trans. Antennas Propagat.*, vol. AP-17, p. 577, Sept. 1969.
- [21] W. T. Shaw and A. J. Dougan, "Half-space Green's functions and applications to scattering of electromagnetic waves from ocean-like surfaces," *Waves in Random Media*, vol. 5, p. 341, July 1995.
- [22] W. T. Shaw, A. J. Dougan, and R. J. A. Tough, "Analytical expressions for correlation functions and Kirchhoff integrals for Gaussian surfaces with ocean-like spectra," *IEEE Trans. Antennas Propagat.*, vol. 44, p. 1454, Nov. 1994.
- [23] W. T. Shaw and A. J. Dougan, "The failure of specular limit formulae for Kirchhoff integrals associated with Gaussian surfaces with ocean-like spectra," *Waves in Random Media*, vol. 5, no. 1, p. L1, Jan. 1995.
- [24] ———, "Curvature corrected impedance boundary conditions in an arbitrary basis," *IEEE Trans. Antennas Propagat.*, to be published.
- [25] B. G. Smith, "Lunar surface roughness: Shadowing and thermal emission," *J. Geophysical Res.*, vol. 72, no. 16, p. 4059, Aug. 1967.
- [26] Spivak, "A numerical approach to rough-surface scattering by the parabolic method," *J. Acoust. Soc. Amer.*, vol. 87, no. 5, p. 1999, May 1990.
- [27] C. T. Tai, *Dyadic Green's Functions in Electromagnetic Theory*, 2nd ed. New York: IEEE Press, 1993.
- [28] V. I. Tatarskii and V. V. Tatarskii, "Statistical description of rough-surface scattering using the quasi-small-slope approximation for random surfaces with a Gaussian multivariate probability distribution," *Waves Random Media*, vol. 4, no. 2, p. 191, Apr. 1994.
- [29] E. I. Thorsos and D. R. Jackson, "Studies of scattering theory using numerical methods," *Waves Random Media*, vol. 1, no. 3, p. S165, July 1991.
- [30] R. J. Tough and K. D. Ward, "Sea surface scattering," 3rd quart. rep., contract LSC/140, TWR/R013/01, TW Res. Ltd., Sept. 1996.
- [31] G. R. Valenzuela, "Depolarization of EM waves by slightly rough surfaces," *IEEE Trans. Antennas Propagat.*, vol. AP-15, p. 552, July 1967.
- [32] A. Voronovich, "Small-slope approximation for electromagnetic wave scattering at a rough interface of two dielectric half-spaces," *Waves Random Media*, vol. 4, no. 3, p. 337, July 1994.
- [33] R. J. Wagner, "Shadowing of randomly rough surfaces," *J. Acoust. Soc. Amer.*, vol. 41, no. 1, p. 138, 1967.
- [34] K. D. Ward, C. J. Baker, and S. Watts, "Maritime surveillance radar—Part 1: Radar scattering from the ocean surface," *Proc. Inst. Elect. Eng.*, vol. 137F, no. 2, p. 51, Apr. 1990.

**William T. Shaw**, for photograph and biography, see p. 1463 of the November 1996 issue of this TRANSACTIONS.

**Andrew J. Dougan**, for photograph and biography, see p. 1463 of the November 1996 issue of this TRANSACTIONS.